EFFECTS OF AIR-DRYING ON THE SHRINKAGE, SURFACE TEMPERATURES AND STRUCTURAL FEATURES OF APPLES SLABS BY MEANS OF FRACTAL ANALYSIS

EFECTOS DEL SECADO CONVECTIVO EN EL ENCOGIMIENTO, TEMPERATURAS SUPERFICIALES Y CARACTERISTICAS ESTRUCTURALES DE PLACAS DE MANZANA MEDIANTE ANALISIS FRACTAL

V. Santacruz-Vázquez [1,2], C. Santacruz-Vázquez [1,2], J. Welti-Chanes [1], R.R. Farrera-Rebollo [1], L. Alamilla-Beltrán [1], J. Chanona-Pérez [1] and G.F. Gutiérrez-López [1,*]

[1] *Escuela Nacional de Ciencias Biológicas–IPN. Departamento de Graduados en Alimentos. Carpio y Plan de Ayala 11340, México, D.F.*
[2] *Benemérita Universidad Autónoma de Puebla, Facultad de Ingeniería Química, Ciudad Universitaria, 72570, Puebla, Pue., México.*

Recibido 13 de Julio 2007; Aceptado 4 de Abril 2008

Abstract

Shrinkage-deformation phenomenon of apple slabs during convective drying was studied, aiming to analyse its causes. Apple slabs were dehydrated in an experimental drying tunnel using a factorial design 4^2. Independent variables were airflow (1, 2, 3 and 4 m/s) and drying air temperature (50, 60, 70 and 80 °C). Relative shrinkage (A/Ao) was evaluated during drying as the ratio of the projected (top view) area of slab at any time during the process (A) to the initial area (Ao) of the same slab. In five punctual measuring zones on the surface of the slab, surface temperatures (ST) and moisture contents (MC) were evaluated. ST and MC were different for each measuring zone, causing irregular dehydration. Fractal analysis was used to evaluate the non-linear (A/Ao) observed pattern and ST distribution. Fractal dimensions for (A/Ao) ratios (FD_A) and ST (FD_{ST}) were 1.08-1.30 and 1.12-1.54 respectively. Temperatures of 60º and 70ºC, and airflows of 2 and 3 m/s caused the highest irregularity of shrinkage and highest FD_A and FD_{ST} values. Scanning electron microscopy images for measuring zone were captured and fractal dimension of texture of images were obtained (FD_{SDBC}) it was observed that non-linear shrinkage was related to irregular microstructure given by FD_{SDBC}.

Keywords: shrinkage-deformation, power law, fractal dimension.

Resumen

Se describe el encogimiento-deformación de placas de manzana durante su deshidratación convectiva y se analizan sus probables causas. La muestras se deshidrataron en un túnel de secado, siguiendo un diseño factorial completo 4^2. Variables: velocidad (1, 2, 3 y 4m/s) y temperatura (50, 60, 70 y 80°C) del aire de secado. Se determinó el encogimiento (A/Ao) de las placas durante la deshidratación. A es el área (vista superior) proyectada de la placa a cualquier tiempo y (Ao) el área inicial. Se determinaron en 5 zonas de medición las temperaturas superficiales (ST) y contenidos de humedad (MC) durante el secado. ST y MC variaron en cada zona causando deshidratación irregular, relacionándose ésto con la no linealidad del encogimiento. Con análisis fractal se evaluó el comportamiento de (A/Ao) y de ST, obteniéndose valores para la dimensión fractal de la relación de áreas (DF_A) y de la distribución de temperaturas superficiales (DF_{ST}) entre 1.08-1.30 y 1.12-1.54 respectivamente. Mayores irregularidades del encogimiento del área y altos valores de DF_A y DF_{ST} se observaron a 60 y 70°C y 2 y 3m/s. Se obtuvieron fotomicrografías de microscopía electrónica de barrido de las zonas seleccionadas y su dimensión fractal de textura (FD_{SDBC}). La no linealidad del encogimiento fue relacionada con la microestructura irregular descrita por FD_{SDBC}.

Palabras clave: encogimiento-deformación, ley de potencia, dimensión fractal.

* *Corresponding autor. E-mail: gusfgl@gmail.com*
Fax: (555) 7296 000 ext. 62463

Publicado por la Academia Mexicana de Investigación y Docencia en Ingeniería Química A.C.

1. Introduction.

Drying or dehydration is one of the most widely used unit operation in food processing. Food drying leads to micro-structural alterations of the products and consequently may affect macroscopic characteristics such as shrinkage (Mattea *et al*., 1989; Mayor & Sereno, 2004). Shrinkage is the reduction in size of a product (macroscopic phenomenon), which for many vegetables is a consequence of the reduction of its cellular dimensions (microscopic phenomena) (Mattea et al., 1989; Krokida & Maroulis, 1997). This phenomenon may cause a negative impression on consumers and can be considered a food quality problem. On the contrary in products such as raisins, amorphous and shrunken appearance is considered as normal.

Several attempts to model the shrinkage of various materials during drying have been reported for starches and seeds (Teotia *et al.*, 1989), garlic (Madamba *et al.*, 1994), apple, carrot and pear (Zogzas *et al*., 1994; Suzuki *et al.*, 1976; Lozano *et al.*, 1980), onion slabs, (Rapusas *et al.*, 1995), stems and leaves (Sokhansanj & Patil, 1996) and apple and potato, (Mulet, 1994; Sjöholm & Gekas, 1995; Wang & Brennan, 1995; Khraisheh *et al.*, 1997). Shrinkage affects mass and heat transfer parameters and is an important factor to be considered when modeling. Most of the studies consider a constant size of the product during drying and consequently the accuracy of the models could be affected (Ramos *et al.*, 2003). Shrinkage is difficult to evaluate given the fact that foodstuffs are not homogeneous and during the first stages of drying they tend to maintain their original shape and as drying continues other phenomena such as deformations, non-isotropic shrinkage and glass transition among other take place (Ratti, 1994; Ratti & Mujumdar, 1995; Yang & Sakai, 2001; Mayor & Sereno, 2004). Fractals have been used to describe and quantify irregular fragments or complex shapes of materials such as shorelines, clouds, plants, brain cells, gold colloids, and sponge iron (Mandelbrot, 1977). Fractal analysis has also been used to study structural and mechanical attributes of some food products. From the particle contours seen in SEM images, Barletta and Barbosa (1993) characterized the ruggedness of instant coffee after agglomeration.

Image and fractal analysis have recently been applied in food research for describing non-linear phenomena during convective drying of food materials (Gutierrez *et al.*, 2002; Chanona *et al.*, 2003; Alamilla *et al.*, 2005) and may also be useful for describing the macroscopic shrinkage of apple slabs. The objective of this paper was to describe, by means of image and fractal analysis, the shrinkage of apple slabs subjected to convective drying.

2. Methodology.

Fresh apples, variety Red Delicious, 88.2±3.4%w/w moisture content and 12.5±1.2 °Bx were purchased at a local market in Puebla City (Mexico). Apples were hand peeled and cut parallel to the main axis using a circular cutter to obtain slabs of parenchyma ($2x10^{-3}$ m thickness and $5x10^{-2}$ m diameter).

2.1 Drying kinetics.

Experiments were carried out in an experimental air drier (Chanona *et al.*, 2003). Drying air temperature and airflow were registered during the process by means of a thermo anemometer Raytek 407112. The effects of drying air temperature (50°, 60°, 70° and 80°C), and airflow (1, 2, 3 and 4 m/s) were studied following a 42 complete factorial design, performing three repetitions for each measurement. Surface temperature (ST) distributions, moisture content (MC) distributions and projected areas (upper-view) (A) of apple slabs were registered during drying kinetics and measured as described in the next section.

2.2. Evaluation of projected areas, moisture content and surface temperatures.

Projected areas (upper-view) of apple slabs during drying were obtained from images recorded with a video camcorder NTSC (Canon, ES400V, USA) (Figure 1a) interfaced to a PC in which images were stored for further analysis. Area of slabs was recorded every 10 minutes of drying kinetics and analyzed by means of the Sigma Scan Image Measurement PRO software (Jandel Scientific Corporation, 2003). The ratio area of slab at any time/maximum area (A/Ao) or normalized area for each image was evaluated at each drying time.

Five measuring punctual zones were selected on the surface of the slabs (Figure 1b) to evaluate moisture content (MC) and superficial temperature (ST). MC in the selected punctual zones was evaluated according to the AOAC 32.1.03 method (A.O.A.C., 1990).

Samples from punctual zones were obtained with a circular cutter in order to obtain small circles (7×10^{-3}m diameter). Moisture content was recorded until the sample reached the equilibrium moisture content. Experiments were carried out by triplicate and the average value for MC was reported.

In order to evaluate ST kinetics for the five measuring punctual zones an infrared thermometer (Raytek, RAYST6LXE, USA) with a laser pointing beam was used. Technical specifications (Raytech allowed to evaluate surface temperature of the slabs in an area of 1 cm^2, considering that the distance from device to spot was 0.07 m (Raytek Infrared Thermometer RAYST6LXE Instruction Manual). Other technical data for the thermometer are: temperature range -32 to 400°C, accuracy ± 0.1°C,

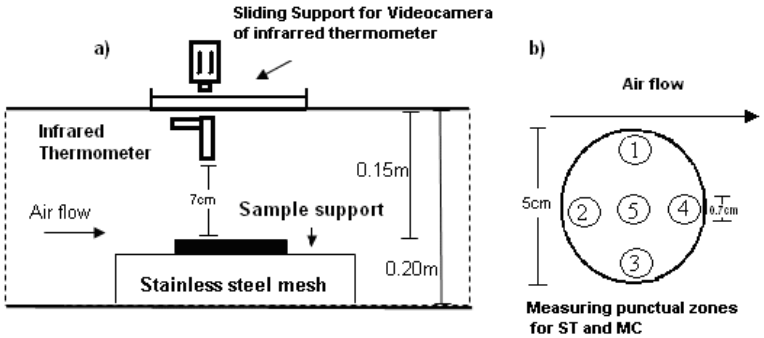

Fig. 1. a) Sectional view of experimental tunnel dryer. b) Measuring punctual zones in apple slices for evaluation of moisture content (MC) and superficial temperature (ST) distribution during drying.

response time 500ms at 95% response, emissivity value 0.93 (suggested by manufacturer as suitable to analyze hot food). ST kinetics were recorded until the ST of slabs reached the dry bulb temperature.

2.3. Power law regressions for (ST) and (A/Ao).

In order to describe the behavior of surface temperatures and normalized projected area during drying, logarithmic plots (ST) and (A/Ao) v_s (1/t) were constructed. The slopes of the resulting curves were used to determine the fractal dimension by means of the method described by Chanona *et al.*, (2003) considering the following expressions:

$$A/Ao \propto (1/t)^{\alpha} \quad (1)$$

$$FD_A = 1+|\alpha| \quad (2)$$

$$ST \propto (1/t)^{\delta} \quad (3)$$

$$FD_{ST} = 1+|\delta| \quad (4)$$

where

$|\alpha|$ = absolute value of the slope of the logarithmic plot (A/Ao) v_s (1/t)

FD_A = fractal dimension of the (A/Ao) ratio during drying.

$|\delta|$ = absolute value of the slope of the logarithmic plot (ST) v_s log (1/t).

FD_{ST}= fractal dimension of (ST) during drying process.

According to Golberg (1992), Chanona, *et al.*, (2003) the fractionary exponents α and δ represented the complexity degree of the kinetics of the ratio (A/Ao) and of ST.

2.4. Fractal texture during convective drying

For the analysis of the structure of the dried samples in the selected punctual zones 2 and 4 (Fig. 1b), a scanning electron microscope was used (JEOL JSM-5900LV Scanning Electron Microscope) at a magnification of 300X. Samples were placed directly on the SEM without treatment. Images were stored as bit-maps in a gray scale with brightness values between 0 and 255. A generalization of the Box Counting method was used to evaluate the fractal dimension of the images. In this work, the shifting differential box-counting method (SDBC) (Wen-Shiung *et al.*, 2003) was used to compute the fractal dimension for the 2-D gray-level of SEM images. For this purpose, the ImageJ 1.34s software (National Institute of Health, NIH, USA) and the codec proposed by Per Henden (Version 1.0, 2006-02-05) were used. The codec is based on an algorithm proposed by Wen-Shiung *et al.* (2003).

All statistical analyses were performed using Minitab 13.1 software (Minitab Inc., Philadelphia State College, USA). A two way analysis of variance ANOVA was applied to evaluate the effect of drying conditions in experimental data of shrinkage (A/Ao), surface temperatures (ST) and fractal texture of SEM photomicrographs (FD_{SDBC}) of apple tissue dried at different conditions. Statistical analysis of Multiple Comparison Procedures was applied on the FD_{SDBC} values, using the Fisher LSD test to determine the presence of significant differences among FD_{SDBC} values.

3. Results and discussion.

3.1. Projected area of apple slabs as a function of drying time.

The projected area of slabs was evaluated as a function of drying time; a reduction of 60% of the original value after 3600 – 7200s was observed. The corresponding reduction in the moisture content varied from 7.33 to 0.25db. It was observed in Figure 2, that the normalized area of the surface (A/Ao) decreases, following an irregular pattern, typical of non-linear functions (Chanona *et al.*, 2003).

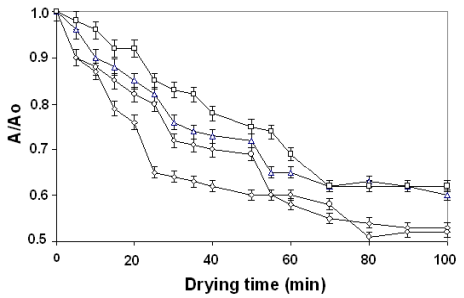

Fig. 2. A/Ao kinetics at different drying conditions (□80°C 2m/s, ◇70°C 2m/s, ○60°C 2m/s, △50°C 2m/s).

The statistical analyses ANOVA reported values of ($P < 0.05$), indicating the temperature and airflow significantly affected the shrinkage of apple slab (A/Ao).

The highest reduction in normalized area was found when drying was carried out using air velocities of 2 and 3 m/s. Gutierrez *et al.*, (2002) used this technique to characterize the distribution of superficial temperatures of a slab of agar slabs during convective drying. The logarithmic plot (A/Ao) v_s (1/t) corresponding to drying kinetic observed at 60°C and 2 m/s is presented in Fig. 3. Three different stages were found in this curve, corresponding to different levels of shrinkage. The first stage, which extends over the first minutes of drying (Fig. 3), presented a lower value of the fractal exponent (slope of the curve) than the second stage, for which non linear behavior of shrinkage (A/Ao) is more pronounced, had duration of 85 min and was the longest drying stage. In the last stage of drying, the change in slope which value was close to zero and no further shrinkage occurs. Given the low values of FD_A during the first stage, it was possible to relate this period with a low degree of deformation. A change of slope of lines in Fig. 3 indicates the onset of stage 2, in which drying continues and moisture and temperature gradients within the slab further influence shrinkage and deformation.

Similar curves to the one reported in Fig. 3 were obtained for other drying conditions. Fractal dimensions for stage 2 for all drying tests are reported in figs. 4 and 5.

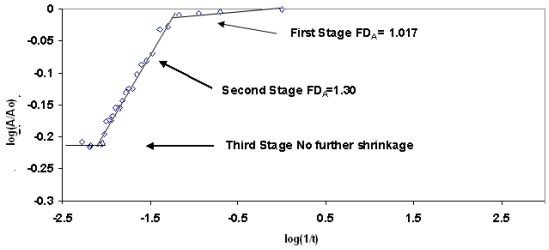

Fig. 3. Log(A/Ao) v_s log(1/t); drying conditions: 60°C and 2m/s.

The drying conditions that produced the highest irregularity in shrinkage and deformation were drying temperatures of 60° and 70ºC, and airflows of 2 and 3 m/s (figs. 4 and 5). At these conditions, distributions of ST and MC in apple slabs generated zones with different moisture contents and temperatures. It is possible to postulate, that the reduction of the dimensions of the slabs is a non-linear phenomenon presenting a more fractal (irregular) behavior at 2 and 3 m/s, and 60° and 70°C. As a consequence, a series of phenomena such as mass transfer processes take place in different directions in the slab causing tension, compression stresses and a consequent non linear behavior in the reduction of the normalized area. The statistical analysis showed that FD_A is significantly ($P < 0.05$) affected by airflow and air temperature as depicted in Fig. 4.

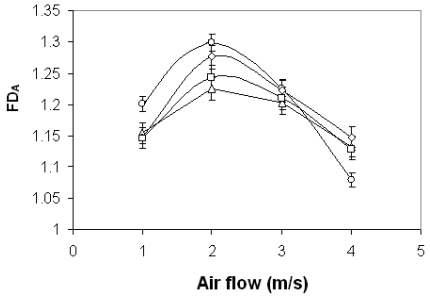

Fig. 4. Effect of airflow during drying of apple slabs on FD_A at different air temperatures (△80°C, ◇70°C, ○60°C, □50°C).

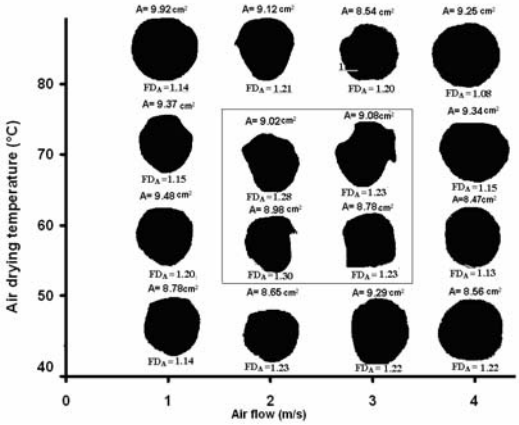

Fig. 5. Binary images of projected area of samples dried under different conditions. Images within square are those for which FD_A was higher.

3.2. Kinetics of surface temperature and moisture content distributions.

Fig. 6a shows the kinetics of superficial temperatures (ST) during drying for the different measuring zones established in methodology (Fig. 1b). At the beginning of drying, the ST distributions in measuring punctual zones were similar between them. However, once drying proceeds, differences in ST among zones became larger, until equilibrium is reached and ST equals dry bulb temperature. Similar ST kinetics to those depicted in Fig. 6a, were observed for other drying conditions and fractal exponents obtained for all ST distribution kinetics were evaluated and reported in the next section.

ST had different values for the five punctual zones, generating thermal gradients on the slab. This may also be caused by internal tensions and heterogeneous distribution of moisture contents in axial and radial directions which may be due to thermomechanical stress and possible presence of deformation and cracking (Hernández-Díaz *et al.* 2008). Similar results have been found by Oliveira *et al.* (1994) during drying of slab-shaped extruded

corn and Lewick *et al.* (2004) for apple slices who reported the presence of tensile effects during convective drying that may induce the moisture and temperature gradients.

Moisture content (MC) distributions in measuring punctual zones are shown in Fig. 6b. Initially, MC values were similar on all punctual zones on the slab and as drying proceeds, differences in MC at the different measuring zones became significant until equilibrium is reached and moisture contents tend to be homogeneous throughout the slab. Evaluated moisture contents on the slab were heterogeneous and presented irregular decreasing patterns during drying. This phenomena has been reported in other works; heterogeneous distribution of moisture contents and temperature on the surface of food slabs was found by Oliveira *et al.* (1994) who reported surface moisture and temperature gradients when convective drying slabs prepared with extruded corn meal with initial moisture content of 0.33 (db). Dry bulb temperatures of drying air used by these authors were 50 and 80°C. They concluded that heterogeneity in the composition of the sample caused internal and surface moisture gradients thus giving place to heterogeneous water flows into and on the slab which are responsible of heterogeneous quality in dried foodstuffs. Lewicki *et al.* (2004) reported mechanical irregularities during the convective drying of apple slabs 15mm in diameter, 5 mm thick. These authors found axial and radial heterogeneous diffusion of water in the samples which caused moisture gradients in both directions giving place to formation of non-isotropic crusts on the material, and presenting irregular moisture distribution moisture causing increased concentrations of solutes that add rigidity to the cell wall. Irregular surface distribution of moisture contents during convective drying have also been reported during drying of green coffee beans in a pilot plant fixed bed drier with transversal airflow; thermomechanical stress and possible presence of deformation and cracking may be responsible of this irregular surface moisture distribution (Hernández-Díaz *et al.*, 2008). Also, Chanona *et al.* (2003) when drying slabs of carbohydrate-based gels 1.5 mm thick, also found surface temperature gradients which were further analyzed by means of power-law regressions.

3.3. Power law regression of superficial temperatures in apple slabs.

Logarithmic plots ST vs. (1/t) were constructed (Fig. 7) according to Chanona *et al.* (2003). Three power-law stages or periods with different slopes were observed for all drying conditions and values of ST fractal exponents for the longest drying stage by means of equation 4, are shown in Fig. 8.

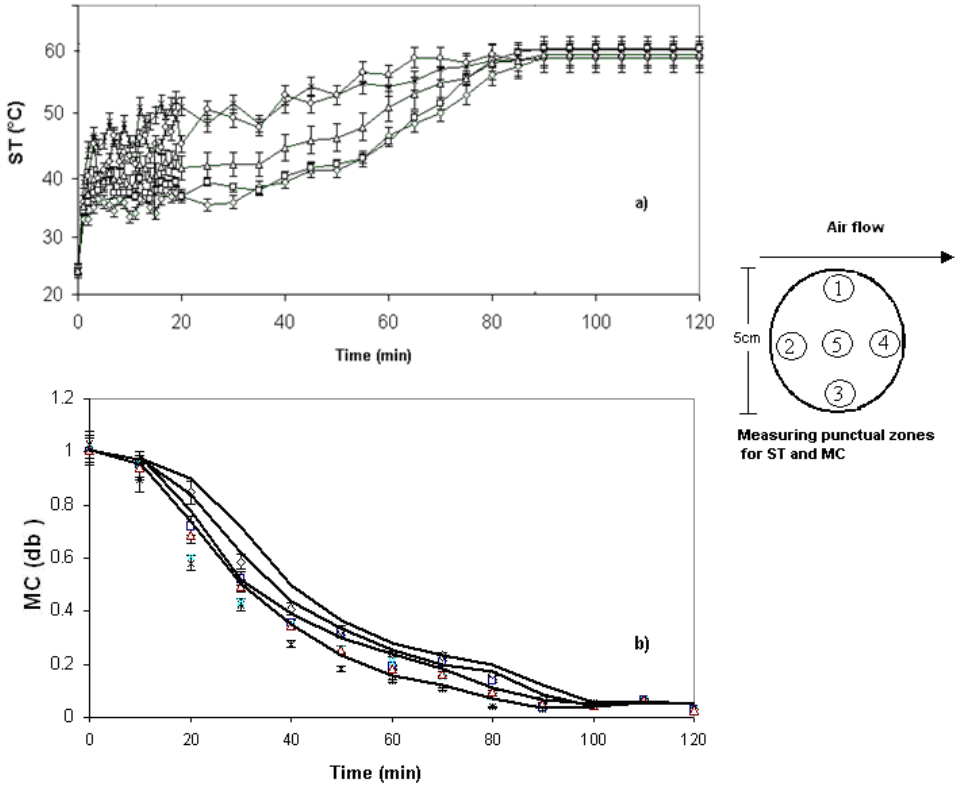

Fig. 6. Distribution of ST and moisture content for punctual zones during drying at 60°C and 2m/s. ○ ZONE 1, ∗ ZONE 2, △ ZONE 3, ◇ZONE 4 and □ ZONE 5.

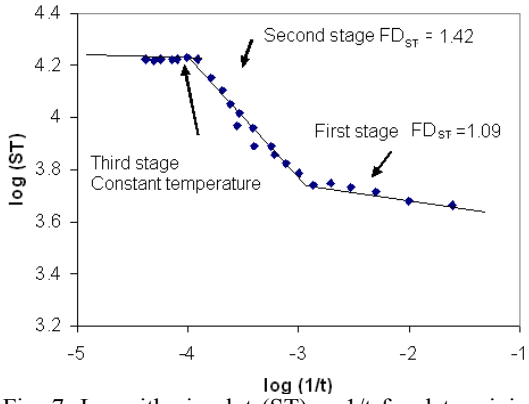

Fig. 7. Logarithmic plot (ST) v_s 1/t for determining the fractal dimension of ST distribution (70°C and 2m/s).

The first stage corresponds to the period in which the thermal profiles were established. This zone had a low value of the slope, and consequently a small value of the fractal dimension. The second stage presented a higher slope as compared to that of the first period and represents most of the drying process. The third stage represents thermal equilibrium and ST tends to homogenize across the sample. The value of the slope for this last stage is consequently, close to zero. Kopelman (1988) when studying fractal order chemical reactions mentioned that systems with fractal dimensions 1<FD<2 represent a distribution of dispersed zones of reacting components on a surface. At airflows of 2 and 3 m/s, the FD_{ST} showed the highest values (Figure 8), indicating that these conditions generated the highest irregularity of the ST and MC distributions, which probably affected slab shrinkage (A/Ao) since at the same conditions, the highest values of FD_A, were also obtained.

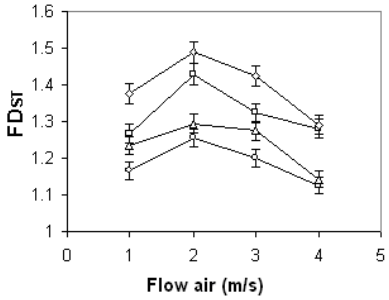

Fig. 8. Fractal dimension of ST distributions of apple slabs during drying at different temperatures: △80°C, □70°C, ◇ 60°C, ○ 50°C.

Statistical analysis showed that airflow and temperatures had significant effects on the values of FD_{ST} ($P < 0.05$). The presence of moisture and thermal gradients may have caused changes on physical and morphological properties as well as water transport profiles which are related to shrinkage and deformation.

3.4. Analysis of microstructure in dried apple tissue.

SEM photomicrographs of apple tissue dried at different conditions corresponding to measuring punctual zone 4 are shown in Fig. 9. Zone 4 was chosen due to the fact that it showed a slower rate of deformation than material at the other zones and was then possible to follow micro-structural changes with more detail.

Samples dried at 50°C showed a deteriorated microstructure due to the effect of dehydration, such as disruption of cell membranes. Also, apple slabs processed at 60°, 70° and 80°C had a notoriously disrupted cell wall as well as the presence of pores and cavities caused by the dehydration process (Figure 9). At low air drying temperatures it is possible to obtain dense products as a result of compact cell walls, while at higher temperatures the increase in porosity and irregularities of cell walls resulted in less dense products which are more porous and rough (Fig. 9).

SEM images of apple slabs subjected to variable airflow are shown in Fig. 9. Tissue dried at 1 and 4 m/s presented less irregular micro-structural patterns as compared to tissue processed at airflows of 2 and 3 m/s. At these conditions, the deformation of structures is more marked, and a non-homogeneous compacting of the cellular structures was evident.

According to FD_{SDBC} values obtained from the micrographs (Fig. 9) it was observed that an increase in drying air temperature produced an increase of FD_{SDBC} values. This tendency indicated that structure became rougher as a consequence of rapid water loss during drying. This may be related to macroscopic shrinkage shown in Fig. 5.

FD_{SDBC} presented the highest values at 2 and 3 m/s, suggesting that the microstructure of the surface of apple gets its roughest structure under these conditions. This may be due to a higher heterogeneity in cellular structure. This heterogeneity was probably due to a quick escape of water and vapor that broke tissues and caused the formation of large pores or tunnels, resulting in relevant structural damage. Tissues dried at mild conditions (50°C, 1 m/s) showed a higher homogeneity in cellular structure as a result of a slower ordered dehydration process (Table 1).

An additional effect of the irregularity of temperature distribution in the tissue (See figs. 9, 10, 11) is the change of microstructure of parenchyma which showed a less compact structure in areas processed at higher superficial temperatures as compared to those dried at lower temperatures. This is particularly evident at punctual zone 2, followed by zones 1 and 3 of apple slabs. Zones 4 and 5 presented the highest cellular compactness.

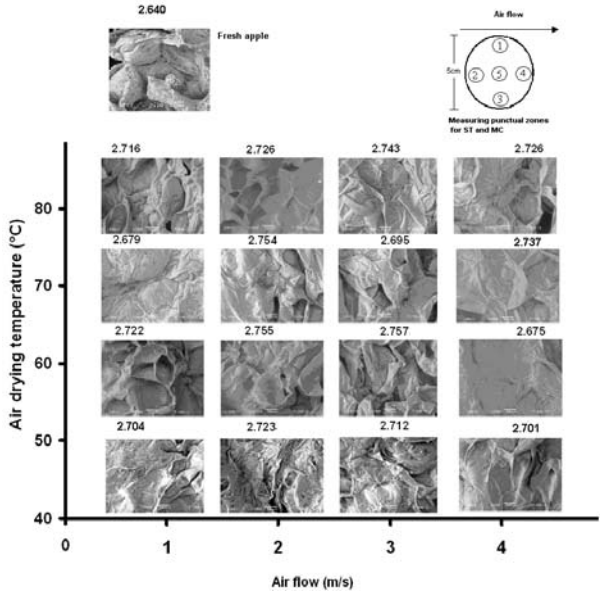

Fig. 9. SEM photomicrographs of apple tissue dried at different conditions in punctual zone 4 and corresponding FD_{SDBC} values.

Table 1. Average values of FD_{SDBC} of photomicrograph SEM of dried apple slabs.

Drying Temperature and Airflow °C-m/s	**FD_{SDBC}**	**Drying Temperature and Airflow °C-m/s**	**FD_{SDBC}**
50°C-1m/s	2.727± 0.0087	70°C -1m/s	2.733± 0.0175
50°C-2m/s	2.733±0.0088	70°C -2m/s	2.766± 0.0169
50°C -3m/s	2.737±0.0075	70°C -3m/s	2.760± 0.0067
50°C -4m/s	2.729±0.0097	70°C -4m/s	2.747± 0.0131
60°C -1m/s	2.749±0.0097	80°C -1m/s	2.726± 0.0134
60°C -2m/s	2.772± 0.0095	80°C -2m/s	2.754± 0.0128
60°C -3m/s	2.764± 0.0027	80°C -3m/s	2.740± 0.0099
60°C -4m/s	2.754± 0.006	80°C -4m/s	2.727± 0.0165

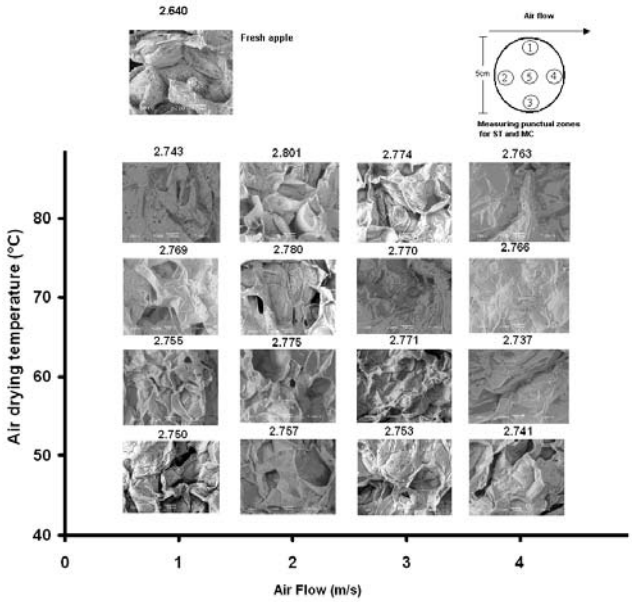

Fig. 10. SEM photomicrographs of apple tissue dried at different conditions in measuring punctual zone 2 and corresponding FD_{SDBC} values.

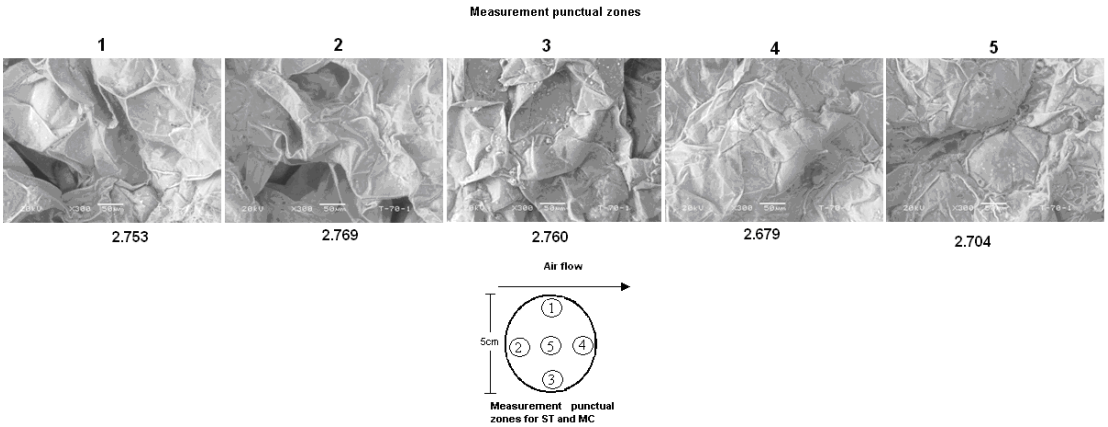

Fig. 11. SEM photomicrographs of apple tissue dried at at 70°C and 1m/s in the indicated measuring punctual zones and corresponding FD_{SDBC} values.

FD_{SDBC} values showed that the roughness of apple slabs tissue is different for each punctual zone, suggesting that the deformation of the tissue during drying is heterogeneous even within the same apple slab (Fig. 11).

Statistical analysis showed that airflow, temperatures and measurement position in slab had significant effects on the values of FD_{SDBC} ($P< 0.05$). The results of statistical analysis of Multiple Comparison showed that at 60° and 70°C and 2 and 3m/s drying conditions produced microstructural modifications, with significant differences in values of FD_{SDBC} (Table 1).

Conclusions

Shrinkage of apple slabs was influenced by, moisture content distribution and micro-structural changes found during drying of apple. A power law with fractional exponents (FD_A and FD_{ST}) higher than one described (A/Ao) and ST kinetics during drying of apple slabs during drying. FD_{SDBC} values obtained from SEM micrographs showed that high drying air temperatures gave place to increased FD_{SDBC} values, indicating a rougher microstructure of the material. Distribution of ST and MC of apple slabs were more heterogeneous when drying took place at 60° and 70°C and 2 and 3m/s this produced higher values of $FD_{A,}$ FD_{ST} and FD_{SDBC} suggesting that in these conditions, temperature/airflow and time of drying influenced deformation and produced non linear macroscopic shrinkage (A/Ao) of apple slabs associated to irregular micro-structural damage. Analysis of SEM photomicrographs of final product demonstrated that drying at 60°C and 70°C, and airflows of 2 and 3m/s gave place to pronounced damage of the apple structure which was also associated to high values of FD_{SDBC} and of $FD_{A,}$ FD_{ST}.

Acknowledgments

We acknowledge the financial support from the PROMEP-SEP program, CONACYT and ENCB-IPN Mexico.

Nomenclature

A	slab projected area, cm^2.
Ao	initial slab projected area, cm^2.
A/Ao	slab normalized projected area
ST	superficial temperature, °C
FD_{ST}	fractal dimension of ST during drying process
FD_A	fractal dimension of normalized projected area during drying process
FD_{SDBC}	fractal dimension for 2-D gray level apple tissue images
MC	moisture contents in selected measuring punctual zones, db
t	drying time
Greek symbols	
$\|\alpha\|$	slope absolute value of the plot log(A/Ao) vs. log(1/t)
$\|\delta\|$	slope absolute value of the plot log(ST) vs. log(1/t)

References

Alamilla, B.L., Chanona, P.J.J., Jiménez, A.A.R. and Gutiérrez, L.G.F. (2005). Description of morphological changes of particles along spray drying. *Journal of Food Engineering 67*(1-2), 179-184.

A.O.A.C. (1990). *Methods of Analysis* (15th ed.). Association of official analytical chemist, Washington, D.C.

Barletta, H.J. and Barbosa, O.G.V. (1993). Fractal analysis to characterize ruggedness changes in tapped agglomerated food powders. *Journal of Food Science 58*(5),1030-1035.

Chanona, J.J., Alamilla, B.L., Farrera, R.F., Quevedo, R., Aguilera, J.M. and Gutiérrez.,

L.G. (2003). Description of the convective air drying of a food model by means of the fractal theory. *Food Science and Technology International 9*(3), 201-207.

Goldberg, A.L. (1992). Fractal mechanisms in the electrophysiology of the heart. *IEEE. Engi in medicine and Biology Magazine. IEEE. Eng. Med. & Bio. 11*, 47-52.

Gutierrez, G.F., Chanona, J.P. and Alamilla, L.B. (2002). A proposal of analysis of the drying phenomena by means of fractal theory. In*: Engineering and Food for the 21st. Century.* (J. Welti-Chanes, G.V. Barbosa-Canovas and J.M. Aguilera, eds.), Pp. 269-287.CRC press, Florida.

Hernández-Díaz, W.N., Ruiz-López, I.I., Salgado-Cervantes, M.A., Rodríguez-Jiménes, G.C. and García- Alvarado, M.A. (2008). Modeling heat and mass transfer during drying of green coffee beans using prolate spheroidal geometry. *Journal of Food Engineering 86*(1), 1-9.

Khraisheh, M.A., Cooper, R. and Magee, T.R.A. (1997). Shrinkage characteristics of potatoes dehydrated under combined and convective air conditions. *Drying Technology 15*(3-4), 1003-1022.

Kopelman, R. (1988). Fractal reaction kinetics. *Science 241*, 1620-1626.

Krokida, M. and Maroulis, Z.B. (1997). Effect of drying method on shrinkage and porosity. *Drying Technology 15*(10), 2441-2458.

Lewicki, P.P. and Jakubczyk, E. (2004). Effect of hot air temperature on mechanical properties of dried apples. *Journal of Food Engineering 64*(1), 307-314.

Lozano, J.E., Rotstein, E. and Urbicain, M.J. (1980). Total porosity and open pore porosity in the drying of fruits. *Journal of Food Science 45*(1), 1403-7.

Madamba, P.S., Driscoll, R.H. and Buckle, K.A. (1994). Shrinkage, density and porosity of garlic during drying. *Journal of Food Engineering 23*(3), 309-319.

Mandelbrot, B.B. (1977). *The fractal geometry of nature*. New York, W.H. Freeman, 30-41.

Mattea, M., Urbicain, M.J. and Rotstein, E. (1989). Computer model of shrinkage and deformation of cellular tissue during dehydration. *Chemical Engineering Science 44*(1), 2853-2859.

Mayor, L. and Sereno, A.M. (2004). Modelling shrinkage during convective drying of food materials: a review. *Journal of Food Engineering 61*(3), 373-386.

Mulet, A. (1994). Drying modelling and water diffusivity in carrots and potatoes. *Journal of Food Engineering 22*(1-4), 329-348.

Oliveira, L.S., Fortes, M. and Haghighl, K. (1994). Conjugate analysis of natural convective drying of biological materials. *Drying Technology 12*(5), 1167-1190.

Ramos, I.N., Brandao, T.R.S. and Silva, C.L. (2003). Structural changes during air drying of fruits and vegetables. *Food Science Technology International 9*(3), 201-206.

Rapusas, R.S., Driscoll, R.H. and Srzednicki, G.S. (1995). Bulk density and resistance to airflow of sliced onions. *Journal of Food Engineering 26*(1), 67-80.

Ratti, C. (1994). Shrinkage during drying of foodstuffs. *Journal of Food Engineering 23*(1), 91-105.

Ratti, C. and Mujumdar, A.S. (1995). Simulation of packed bed drying of foodstuffs with airflow reversal. *Journal of Food Engineering 26*(3), 259-271.

Sjöholm, I. and Gekas, V. (1995). Apple shrinkage upon drying. *Journal of Food Engineering 25* (1), 123-130.

Sokhansanj, S. and Patil R.T. (1996) Kinetics of dehydration of green alfalfa. *Drying Technology 14*(5), 1197-1234.

Suzuki, K., Kubota, K., Hasegawa, T. and Osaka, H. (1976) Shrinkage in dehydration of root vegetables. *Journal of Food Science 41*(1), 1189-93.

Teotia, M.S. and Ramakrishna, P. (1989). Research note: Densities of melon seeds, kernels and hulls. *Journal of Food Engineering 9*(3), 231-236.

Wang, N. and Brennan, J.G. (1995). Changes in structure, density and porosity of potato during dehydration. *Journal of Food Engineering 24*(1), 61-76.

Wen-Shiung, Ch., Shang-Yuan, Y. and Chih-Ming, H. (2003). Two algorithms to estimate fractal dimension of gray-level images. *Optical Engineering 42*(8), 2452-2464.

Yang, Y. and Sakai, R. (2001). Drying model with shrinkage undergoing simultaneous heat and mass transfer. In: *Proceedings of the 8th International Congress on Engineering and Food. Puebla, México, 2001,* (J. Welti-Chanes, G.V. Barbosa-Canovas and J.M. Aguilera, eds.), Pp. 1100-1005. Technomic Publishing Co. Pennsylvania.

Zogzas, N.P., Maroulis, Z.B., Marinos-Houris, D. and Saravacos, G.D. (1994). Densities shrinkage and porosity of some vegetables during air drying. In: *Drying 94,* (R.V. Keey and R.B., Mujumdar, eds.), Pp. 863-870. Chapman.